

World Journal of *Radiology*

World J Radiol 2023 August 28; 15(8): 241-255



ORIGINAL ARTICLE

Retrospective Study

- 241 Appearance of aseptic vascular grafts after endovascular aortic repair on [(18)F]fluorodeoxyglucose positron emission tomography/computed tomography

Bennett P, Tomas MB, Koch CF, Nichols KJ, Palestro CJ

CASE REPORT

- 250 Rare portal hypertension caused by Abernethy malformation (Type IIC): A case report

Yao X, Liu Y, Yu LD, Qin JP

ABOUT COVER

Editorial Board Member of *World Journal of Radiology*, Francesco Lassandro, MD, Doctor, Medical Assistant, Radiology Section, Department of Services, Azienda Ospedali dei Colli, Monaldi Hospital, Naples 80131, Italy. f.lassandro@gmail.com

AIMS AND SCOPE

The primary aim of *World Journal of Radiology (WJR, World J Radiol)* is to provide scholars and readers from various fields of radiology with a platform to publish high-quality basic and clinical research articles and communicate their research findings online.

WJR mainly publishes articles reporting research results and findings obtained in the field of radiology and covering a wide range of topics including state of the art information on cardiopulmonary imaging, gastrointestinal imaging, genitourinary imaging, musculoskeletal imaging, neuroradiology/head and neck imaging, nuclear medicine and molecular imaging, pediatric imaging, vascular and interventional radiology, and women's imaging.

INDEXING/ABSTRACTING

The *WJR* is now abstracted and indexed in PubMed, PubMed Central, Emerging Sources Citation Index (Web of Science), Reference Citation Analysis, China National Knowledge Infrastructure, China Science and Technology Journal Database, and Superstar Journals Database. The 2023 Edition of Journal Citation Reports® cites the 2022 impact factor (IF) for *WJR* as 2.5; IF without journal self cites: 2.3; 5-year IF: 2.5; Journal Citation Indicator: 0.54.

RESPONSIBLE EDITORS FOR THIS ISSUE

Production Editor: *Si Zhao*; Production Department Director: *Xu Guo*; Editorial Office Director: *Jia-Ping Yan*.

NAME OF JOURNAL

World Journal of Radiology

ISSN

ISSN 1949-8470 (online)

LAUNCH DATE

January 31, 2009

FREQUENCY

Monthly

EDITORS-IN-CHIEF

Thomas J Vogl

EDITORIAL BOARD MEMBERS

<https://www.wjgnet.com/1949-8470/editorialboard.htm>

PUBLICATION DATE

August 28, 2023

COPYRIGHT

© 2023 Baishideng Publishing Group Inc

INSTRUCTIONS TO AUTHORS

<https://www.wjgnet.com/bpg/gerinfo/204>

GUIDELINES FOR ETHICS DOCUMENTS

<https://www.wjgnet.com/bpg/GerInfo/287>

GUIDELINES FOR NON-NATIVE SPEAKERS OF ENGLISH

<https://www.wjgnet.com/bpg/gerinfo/240>

PUBLICATION ETHICS

<https://www.wjgnet.com/bpg/GerInfo/288>

PUBLICATION MISCONDUCT

<https://www.wjgnet.com/bpg/gerinfo/208>

ARTICLE PROCESSING CHARGE

<https://www.wjgnet.com/bpg/gerinfo/242>

STEPS FOR SUBMITTING MANUSCRIPTS

<https://www.wjgnet.com/bpg/GerInfo/239>

ONLINE SUBMISSION

<https://www.f6publishing.com>

Retrospective Study

Appearance of aseptic vascular grafts after endovascular aortic repair on [(18)F]fluorodeoxyglucose positron emission tomography/computed tomography

Paige Bennett, Maria Bernadette Tomas, Christopher F Koch, Kenneth J Nichols, Christopher J Palestro

Specialty type: Radiology, nuclear medicine and medical imaging**Provenance and peer review:** Invited article; Externally peer reviewed.**Peer-review model:** Single blind**Peer-review report's scientific quality classification**Grade A (Excellent): 0
Grade B (Very good): B, B
Grade C (Good): 0
Grade D (Fair): 0
Grade E (Poor): 0**P-Reviewer:** Covantsev S, Russia;
Long X, China**Received:** March 28, 2023**Peer-review started:** March 28, 2023**First decision:** June 1, 2023**Revised:** June 15, 2023**Accepted:** July 27, 2023**Article in press:** July 27, 2023**Published online:** August 28, 2023**Paige Bennett**, Department of Radiology, LIJMC Northwell Health, New Hyde Park, NY 11040, United States**Paige Bennett, Maria Bernadette Tomas, Kenneth J Nichols, Christopher J Palestro**, Department of Radiology, Zucker School of Medicine at Hofstra/Northwell, Hempstead, NY 11549, United States**Christopher F Koch**, Division of Nuclear Medicine and Molecular Imaging, Department of Radiology, Northwell Health, New Hyde Park, NY 11040, United States**Corresponding author:** Paige Bennett, MD, Professor, Department of Radiology, LIJMC Northwell Health, Rm C204, 27005 76th Avenue, New Hyde Park, NY 11040, United States.pbennett1@northwell.edu

Abstract

BACKGROUND

Diagnosis of prosthetic vascular graft infection with [(18)F]fluorodeoxyglucose positron emission tomography/computed tomography (18F-FDG PET/CT) allows for early detection of functional changes associated with infection, based on increased glucose utilization by activated macrophages and granulocytes. Aseptic vascular grafts, like all foreign bodies, can stimulate an inflammatory response, which can present as increased activity on 18F-FDG PET/CT. Consequently, distinguishing aseptic inflammation from graft infection, though important, can be difficult. In the case of endovascular aneurysm repair (EVAR), a minimally invasive procedure involving the transfemoral insertion of an endoprosthetic stent graft, the normal postoperative appearance of these grafts on 18F-FDG PET/CT can vary over time, potentially confounding study interpretation.

AIM

To investigate the visual, semiquantitative, and temporal characteristics of aseptic vascular grafts in patients status post EVAR.

METHODS

In this observational retrospective cohort study, patients with history of EVAR who underwent 18F-FDG PET/CT for indications other than infection were

identified retrospectively. All patients were asymptomatic for graft infection - no abdominal pain, fever of unknown origin, sepsis, or leukocytosis - at the time of imaging and for ≥ 2 mo after each PET/CT. Imaging studies such as CT for each patient were also reviewed, and any patients with suspected or confirmed vascular graft infection were excluded. One hundred two scans performed on 43 patients (34 males; 9 females; age = 77 ± 8 years at the time of the final PET/CT) were retrospectively reviewed. All 43 patients had an abdominal aortic (AA) vascular graft, 40 patients had a right iliac (RI) limb graft, and 41 patients had a left iliac (LI) limb graft. Twenty-two patients had 1 PET/CT and 21 patients had from 2 to 9 PET/CTs. Grafts were imaged between 2 mo to 168 mo (about 14 years) post placement. Eight grafts were imaged within 6 mo of placement, including three that were imaged within three months of placement. The mean interval between graft placement and PET/CT for all 102 scans was 51 ± 39 mo. PET/CT data was reconstructed with region-of-interest analysis of proximal, mid and distal portions of the grafts and background ascending aorta. Maximum standardized uptake value (SUV_{max}) was recorded for each region. SUV_{max} -to-background uptake ratios (URs) were calculated. Visual assessment was performed using a 2-pattern grading scale: Diffuse (homogeneous uptake less than liver uptake) and focal (one or more areas of focal uptake in any part of the graft). Statistical analysis was performed.

RESULTS

In total, there were 306 AA grafts, 285 LI grafts, 282 RI grafts, and 306 ascending aorta background SUV_{max} measurements. For all 102 scans, mean SUV_{max} values for AA grafts were 2.8-3.0 along proximal, mid, and distal segments. Mean SUV_{max} values for LI grafts and RI grafts were 2.7-2.8. Mean SUV_{max} values for background were 2.5 ± 0.5 . Mean URs were 1.1-1.2. Visual analysis of the scans reflected results of quantitative analysis. On visual inspection, 98% revealed diffuse, homogeneous 18F-FDG uptake less than liver. Graft URs and visual pattern categories were significantly associated for AA graft URs (F-ratio = 21.5, $P < 0.001$), LI graft URs (F-ratio = 20.4, $P < 0.001$), and RI graft URs (F-ratio = 30.4, $P < 0.001$). Thus, visual patterns of 18F-FDG uptake corresponded statistically significantly to semiquantitative URs. The age of grafts showing focal patterns was greater than grafts showing diffuse patterns, 87 ± 89 vs 50 ± 37 mo, respectively ($P = 0.02$). URs were significantly associated with graft age for AA grafts ($r = 0.19$, $P = 0.001$). URs were also significantly associated with graft age for LI grafts ($r = 0.25$, $P < 0.0001$), and RI grafts ($r = 0.31$, $P < 0.001$). Quartiles of similar numbers of graft ($n = 25-27$) grouped by graft age indicated that URs were significantly higher for 4th quartile vs 2nd quartile URs (F-ratio = 19.5, $P < 0.001$). When evaluating URs, graft SUV_{max} values within 10%-20% of the ascending aorta SUV_{max} is evident in aseptic grafts, except for grafts in the oldest quartiles. In this study, grafts in the oldest quartiles (> 7 years post EVAR) showed SUV_{max} up to 30% higher than the ascending aorta SUV_{max} .

CONCLUSION

Characteristics of an aseptic vascular stent graft in the aorta and iliac vessels on 18F-FDG PET/CT include graft SUV_{max} values within 10%-20% of the ascending aorta background SUV_{max} . The SUV_{max} of older aseptic grafts can be as much as 30% above background. The visual uptake pattern of diffuse, homogeneous uptake less than liver was seen in 98% of aseptic vascular grafts, making this pattern particularly reassuring for clinicians.

Key Words: Aseptic vascular grafts; Endovascular aortic repair; [(18)F]fluorodeoxyglucose positron emission tomography/computed tomography

©The Author(s) 2023. Published by Baishideng Publishing Group Inc. All rights reserved.

Core Tip: In patients post endovascular aortic repair who undergo [(18)F]fluorodeoxyglucose positron emission tomography/computed tomography, aseptic vascular grafts show maximum standardized uptake value (SUV_{max}) within 10%-20% of background ascending aorta SUV_{max} values. Older aseptic vascular grafts can show up to 30% higher uptake vs background compared with younger aseptic vascular grafts. The visual uptake pattern of diffuse, homogeneous uptake less than liver was seen in 98% of aseptic vascular grafts, making this pattern particularly reassuring for clinicians.

Citation: Bennett P, Tomas MB, Koch CF, Nichols KJ, Palestro CJ. Appearance of aseptic vascular grafts after endovascular aortic repair on [(18)F]fluorodeoxyglucose positron emission tomography/computed tomography. *World J Radiol* 2023; 15(8): 241-249

URL: <https://www.wjgnet.com/1949-8470/full/v15/i8/241.htm>

DOI: <https://dx.doi.org/10.4329/wjr.v15.i8.241>

INTRODUCTION

Diagnosis of prosthetic vascular graft infection with [(18)F]fluorodeoxyglucose positron emission tomography/computed tomography (18F-FDG PET/CT) allows for detection of early functional changes associated with infection, based on

increased glucose utilization by activated macrophages and granulocytes. 18F-FDG PET/CT can be an important diagnostic adjunct to CT, which depends on anatomic changes, such as perigraft air, fluid, soft tissue, fistula, and abscess for diagnosis of infection. However, sterile vascular grafts, like all foreign bodies, can stimulate an aseptic inflammatory response that presents as increased activity on 18F-FDG PET/CT. Consequently, distinguishing aseptic inflammation from vascular graft infection can be difficult, and standardized interpretation criteria for differentiating between these two conditions have not been universally adopted[1].

Currently, medical literature supports diagnostic sensitivity and specificity of 18F-FDG PET/CT in diagnosing vascular graft infection of 89%-98% and 59%-81%, respectively[2,3]. Note that the lower specificity raises the possibility of false-positive interpretations of 18F-FDG uptake on PET/CT. This has important clinical consequences, including unnecessary long-term antibiotic therapy, invasive procedures, and potential for graft explantation which carries an 18%-30% mortality rate due to complications[1,4,5]. As the negative predictive value of 18F-FDG PET/CT for excluding vascular graft infection is high (about 93%), the expected physiological patterns of 18F-FDG uptake in uninfected vascular grafts should be identified to avoid false-positive interpretation[4,6].

However, evidence on the appearance of aseptic vascular grafts over time on 18F-FDG PET/CT is sparse, maximum standardized uptake value (SUV_{max}) cutoff values for aseptic grafts have not been clearly defined, and visual pattern analysis is often suggested to distinguish aseptic from infected vascular grafts[2,7-10]. In the case of endovascular aneurysm repair (EVAR), a minimally invasive procedure involving the transfemoral insertion of an endoprosthetic stent graft, the normal postoperative appearance of these grafts on 18F-FDG PET/CT can vary over time, potentially confounding study interpretation[11,12]. Thus, this study was performed to evaluate visual, semiquantitative, and temporal characteristics of aseptic endovascular aneurysm grafts on 18F-FDG PET/CT.

MATERIALS AND METHODS

Patients

In this observational retrospective cohort study, patients with history of EVAR who underwent 18F-FDG PET/CT for indications other than infection were identified retrospectively. All patients were asymptomatic for graft infection - no abdominal pain, fever of unknown origin, sepsis, or leukocytosis - at the time of imaging and for ≥ 2 mo after each PET/CT. Imaging studies such as CT for each patient were also reviewed, and any patients with suspected or confirmed vascular graft infection were excluded. One hundred two scans performed on 43 patients (34 males; 9 females; age = 77 ± 8 years at the time of the final PET/CT) were retrospectively reviewed. All 43 patients had an abdominal aortic (AA) vascular graft, 40 patients had a right iliac (RI) limb graft, and 41 patients had a left iliac (LI) limb graft. Twenty-two patients had 1 PET/CT and 21 patients had from 2 to 9 PET/CTs. Grafts were imaged between 2 mo to 168 mo (about 14 years) post placement. Eight grafts were imaged within 6 mo of placement, including three that were imaged within three months of placement. The mean interval between graft placement and PET/CT for all 102 scans was 51 ± 39 mo. Types of graft material were obtained from the patients' medical records, when available ($n = 19$). The Institutional Review Board approved this retrospective study and the requirement to obtain informed consent was waived. All data were handled in compliance with the Health Insurance Portability and Accountability Act of 1996.

Data acquisition

Data were acquired on 4 PET/CT systems: 2 Siemens Biograph mCT 64 (Munich, Germany) and 2 GE D710 (GE Healthcare, Chicago, IL, United States) systems. Data were reconstructed using manufacturer recommended 18F-FDG PET/CT reconstruction parameters on associated workstations at which data were acquired.

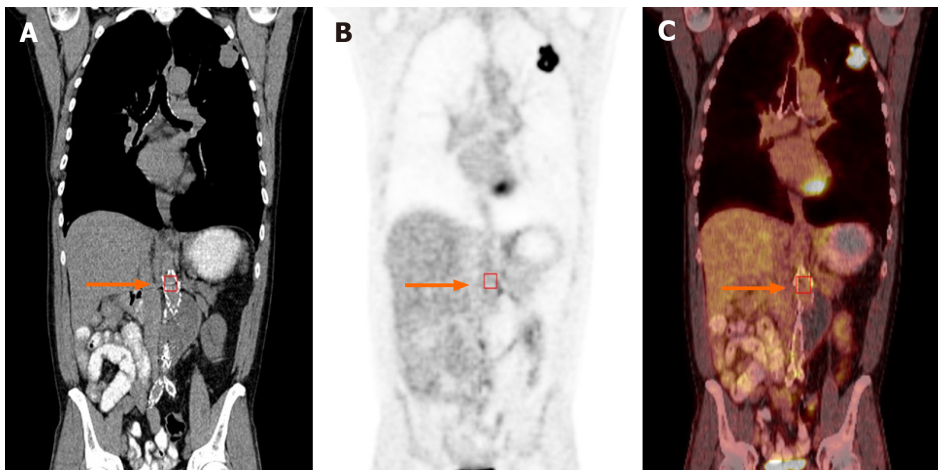
Image analysis

All reconstructed data were reviewed on a single GE AW workstation (GE Healthcare, Chicago, IL, United States). One nuclear medicine physician (MBT) analyzed all PET/CT images and obtained semiquantitative SUV_{max} using manually drawn region of interest (ROI) analysis. For each graft, a square ROI was drawn encompassing the width of the graft, cross-referenced on CT and confirmed on fused PET/CT images (Figure 1). ROIs were drawn around the proximal, mid, and distal portions of the AA graft, and SUV_{max} was recorded for each region. A similar ROI was used to measure SUV_{max} in the ascending aorta as the background (BKG) reference. SUV_{max} was also measured at proximal, mid, and distal portions of the RI and LI grafts when present. ROIs for each of the 3 locations along the grafts were placed equidistant.

Analyses were performed for SUV_{max} values to avoid underrepresentation of 18F-FDG uptake that could result from sampling tissue outside of graft tissues. To avoid the possibility of different PET/CT systems or software generating SUV_{max} values that were different from one another, the uptake ratio (UR) of SUV_{max} was calculated for each graft location using the formula: $UR = SUV_{max} \text{ graft} / SUV_{max} \text{ BKG}$. The URs were analyzed to minimize effects of using different PET/CT systems and image reconstruction algorithms.

Visual assessment

The same nuclear medicine physician who placed ROIs for semiquantitative analysis also classified uptake according to two visual patterns for aseptic grafts: Diffuse and focal. Diffuse was defined as mild, homogeneous uptake less than liver. Focal was defined as one or more areas of focal uptake in any part of the graft. Reference for visual analysis was 18F-FDG uptake in the liver.



DOI: 10.4329/wjr.v15.i8.241 Copyright ©The Author(s) 2023.

Figure 1 Coronal [(18)F]fluorodeoxyglucose positron emission tomography/computed tomography showing example of region of interest analysis on an abdominal aortic graft (arrow). A: Non-contrast computed tomography (CT); B: Positron emission tomography (PET); C: Fused PET/CT images.

Statistical analysis

Analyses were performed using commercially available software (“MedCalc” Statistical Software version 20.110; MedCalc Software Ltd, Ostend, Belgium; <https://www.medcalc.org>; 2022). Values were reported as mean \pm SD. The Kolmogorov-Smirnov method assessed whether continuous variables were normally distributed and provided means and distribution percentiles. ANOVA with Bonferroni correction compared SUV_{max} and URs grouped by age of grafts, ROI locations, and graft material. Significance of differences between mean values were assessed by the unpaired student’s *t*-test for normally distributed variables and by the Mann-Whitney test for non-normally distributed variables. Significance of changes over time was determined by linear regression of URs *vs* graft age. Linear regression of URs *vs* the time difference from the first through the last scan was performed for each patient with more than 1 PET/CT. Also, a separate subgroup analysis of patients with 3 or more scans was performed similarly with URs compared with the time difference from the first through the last scan of each patient. The Tukey test was applied to URs to detect outliers. For all tests, $P < 0.05$ was defined as statistically significant, or as adjusted by Bonferroni corrections for comparisons among multiple categories.

RESULTS

In total, there were 306 AA grafts, 285 LI grafts, 282 RI grafts, and 306 BKG SUV_{max} measurements. For all 102 scans, mean SUV_{max} values for AA grafts were 2.8-3.0 along proximal, mid, and distal segments (Table 1). Mean SUV_{max} values for LI grafts and RI grafts were 2.7-2.8. Mean SUV_{max} values for BKG were 2.5 ± 0.5 (Table 2). Mean URs were 1.1-1.2 (Tables 1 and 2).

Of the 43 patients, graft material was identifiable for 10 patients who had polyethylene terephthalate (PT) grafts and 9 patients who had polytetrafluoroethylene (PTFE) grafts. There were 87 SUV_{max} measurements of PT grafts and 78 SUV_{max} measurements of PTFE grafts. ANOVA indicated a modest difference (F-ratio = 5.1, $P = 0.03$) of AA graft URs between PT and PTFE graft materials (1.2 ± 0.3 *vs* 1.1 ± 0.2 , $P = 0.03$).

URs were significantly associated with graft age for AA grafts ($r = 0.19$, $P = 0.001$) (Figure 2). URs were also significantly associated with graft age for LI grafts ($r = 0.25$, $P < 0.0001$), and RI grafts ($r = 0.31$, $P < 0.001$). Quartiles of similar numbers of graft ($n = 25-27$) grouped by graft age indicated that URs were significantly higher for 4th quartile *vs* 2nd quartile URs (F-ratio = 19.5, $P < 0.001$) (Table 3). URs were similar for patients for whom graft placement was < 3 mo *vs* those with older grafts and were likewise similar for patients for whom graft placement was < 6 mo *vs* those with older grafts (F-ratio < 2.0 , $P > 0.05$). While correlation of URs versus graft age was significant for all AA grafts (Figure 2), when analyzed separately by location, strongest correlation *vs* AA graft age was for proximal ROIs, less strong for mid ROIs, and not significant for distal ROIs (Figure 3). The highest UR value (2.89) corresponded to the patch region of the graft in one patient.

Patients with multiple PET/CT studies

A total of 80 18F-FDG PET/CTs were performed on the 21 patients with repeat scans: 5 patients had 2; 8 patients had 3; 3 patients had 4; 3 patients had 6; 1 patient had 7; and 1 patient had 9 scans. Correlations of URs over time from the first through the last scan were not significant ($r = 0.10$, $P = 0.09$) (Figure 4). There were 210 URs evaluated for the subgroup of patients with 3 or more scans. For this subgroup, URs were not correlated with time from the first through the last scan ($r = 0.12$, $P = 0.07$).

Table 1 Maximum standardized uptake value and uptake ratios for aortic graft locations

Location	SUV _{max}	Uptake ratio
Proximal aortic graft	2.8 ± 0.8	1.1 ± 0.3
Mid aortic graft	2.9 ± 0.8	1.2 ± 0.3
Distal aortic graft	3.0 ± 0.9	1.2 ± 0.3
Background	2.5 ± 0.5	-

SUV_{max}: Maximum standardized uptake value.

Table 2 Maximum standardized uptake value for grafts and background (ascending aorta), uptake ratios are listed for grafts

Location	SUV _{max}	Uptake ratio
Aortic graft	2.9 ± 0.8	1.2 ± 0.3
Left Iliac graft	2.7 ± 0.8	1.1 ± 0.3
Right Iliac graft	2.8 ± 0.8	1.2 ± 0.4
Background	2.5 ± 0.5	-

SUV_{max}: Maximum standardized uptake value.

Table 3 Graft age and uptake ratios segregated into quartiles by graft age

Graft, age, quartile	Graft age (mo)	Uptake ratio		
		Aortic graft	L-iliac graft	R-iliac graft
1	9 ± 4	1.2 ± 0.2	1.1 ± 0.2 ^a	1.1 ± 0.2 ^a
2	31 ± 10	1.1 ± 0.2 ^a	1.1 ± 0.2 ^a	1.1 ± 0.2 ^a
3	60 ± 9	1.1 ± 0.3 ^a	1.1 ± 0.3 ^a	1.1 ± 0.4 ^a
4	107 ± 24	1.3 ± 0.3	1.3 ± 0.4	1.4 ± 0.4

^aP < 0.05 versus graft age quartile #4.

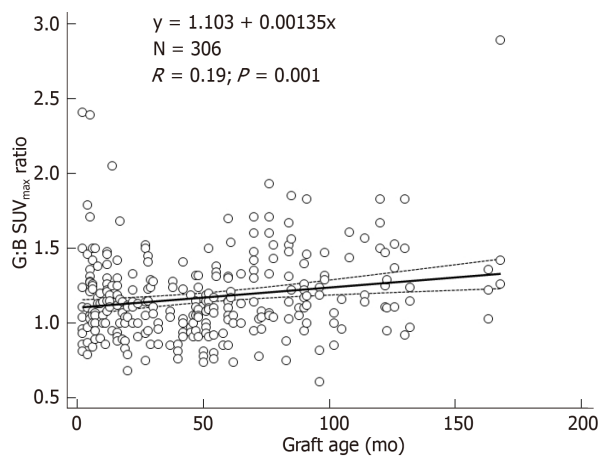


Figure 2 Graft uptake ratios vs graft age in months for abdominal aortic grafts. SUV_{max}: Maximum standardized uptake value.

Visual analyses

Visual analysis of the scans reflected results of quantitative analysis (Table 4). On visual inspection, 98% revealed diffuse, homogeneous 18F-FDG uptake less than liver. Graft URs and visual pattern categories were significantly associated for AA graft URs (F-ratio = 21.5, $P < 0.001$), LI graft URs (F-ratio = 20.4, $P < 0.001$), and RI graft URs (F-ratio = 30.4, $P < 0.001$). Thus, visual patterns of 18F-FDG uptake corresponded statistically significantly to semiquantitative URs. The age of grafts showing focal patterns was greater than grafts showing diffuse patterns, 87 ± 89 vs 50 ± 37 mo, respectively ($P = 0.02$).

Visual uptake patterns were similar for different graft materials, when known, in that similar percentages of PT grafts and PTFE grafts were scored with focal visual patterns (2% vs 1%, $P = 0.63$) (Table 5), and similar to the 2% (6/306) of focal visual patterns for all grafts (Table 4).

Tests for outliers

The Tukey test showed there were 3 outlier cases for 3 different patients among the 306 graft URs. Even after excluding these 3 cases, there was significant association with URs and graft age for AA graft URs ($r = 0.19$, $P = 0.001$) (Figure 2). Similarly, there was significant association with URs and graft age for LI graft URs ($r = 0.25$, $P < 0.001$) and RI graft URs ($r = 0.31$, $P < 0.001$). Thus, no results were altered by excluding the 3 outliers.

DISCUSSION

In this study, the 18F-FDG PET/CT appearance of aseptic vascular grafts was delineated on 43 patients post EVAR without clinical signs and symptoms of vascular graft infection who underwent 18F-FDG PET/CT for oncologic indications. Visual, semiquantitative SUV_{max} and graft-to-background UR analysis was performed for 306 AA grafts, 285 LI grafts and 282 RI grafts. To our knowledge, this is the largest analysis of aseptic vascular graft appearance on 18F-FDG PET/CT to date.

All patients with aseptic aortic and iliac grafts showed graft SUV_{max} values of 3 or below. This is supported by a study by Tsuda *et al*[13] showing SUV_{max} below 4.5 in uninfected grafts, which was not dependent on time after surgery or whether the graft was placed in an open or endovascular fashion. Other studies have reported SUV_{max} values greater than 3.8-4.5 as significant for infection, which is supported by this study showing lower SUV_{max} values in aseptic grafts[14,15].

As SUV_{max} values can vary based on differences in PET/CT scanners, reconstruction algorithms and quality control efforts, we chose to include graft-to-background URs in our analyses. When evaluating URs, graft SUV_{max} values within 10%-20% of the ascending aorta SUV_{max} is evident in aseptic grafts, except for grafts in the oldest quartiles. In this study, grafts in the oldest quartile (> 7 years post EVAR) showed SUV_{max} up to 30% higher than the ascending aorta SUV_{max} .

The highest difference in URs was evident in PT grafts compared to PTFE grafts, although this modest difference is likely not clinically significant (1.2 ± 0.3 vs 1.1 ± 0.2 , $P = 0.03$). When vascular grafts are encountered in the PET/CT clinic, two measurements of the ascending aorta and the graft can help to confirm a clinically noninfected appearance.

Visual analysis of vascular grafts in these patients was useful to detect a diffuse, homogeneous pattern of 18F-FDG uptake less than liver uptake, with results comparable to semiquantitative SUV_{max} and UR analysis. This suggests that visual comparison to the liver during image evaluation can be used to confirm a noninfected graft. The uptake pattern of 18F-FDG in aseptic vascular grafts was usually diffuse (300/306 = 98%), making this pattern particularly reassuring for clinicians.

When considering graft age, our data show a tendency for older grafts to exhibit higher 18F-FDG uptake. Those in the oldest quartile of the study (mean age 107 ± 24 mo) had mean URs of 1.3-1.4. Grafts in the lower 3 graft-age quartiles had mean URs closer to 1.1. Therefore, clinicians should consider the possibility of graft SUV_{max} being as much as 30% above ascending aorta background for old vascular grafts, particularly in proximal graft regions.

Limitations of this study include its retrospective nature, with chart review analysis the only means available to confirm absence of vascular graft infection in these patients. In addition, not all patients had contrast-enhanced CT for correlation with presence or absence of findings of vascular graft infection on anatomic imaging. Information regarding graft material composition was not available on all patients, potentially limiting analysis based on graft material. Another limitation is that a sole reader evaluated all data points on the PET/CT scans, including SUV_{max} and visual analysis. Therefore, interobserver variability in interpretation was not analyzed. Finally, our study did not include analysis of 18F-FDG PET/CT in patients with suspected or confirmed vascular graft infections, to compare with findings in aseptic vascular grafts in a similar patient population.

CONCLUSION

For 18F-FDG PET/CT interpreters, the visual, semiquantitative, and temporal characteristics of aseptic vascular stent grafts in patients' status post EVAR can be useful in interpreting PET/CT, whether stent grafts are encountered as incidental findings on oncologic scans or on scans performed for suspected vascular graft infection. Our findings reinforce prior research in determining the characteristics of aseptic vascular grafts in a large cohort of grafts analyzed over time.

Table 4 Frequency of visual uptake patterns for all grafts and uptake ratios

Visual uptake pattern	<i>n</i>	Uptake ratio
Diffuse	300	1.1 ± 0.3
Focal	6	1.8 ± 0.7 ^a

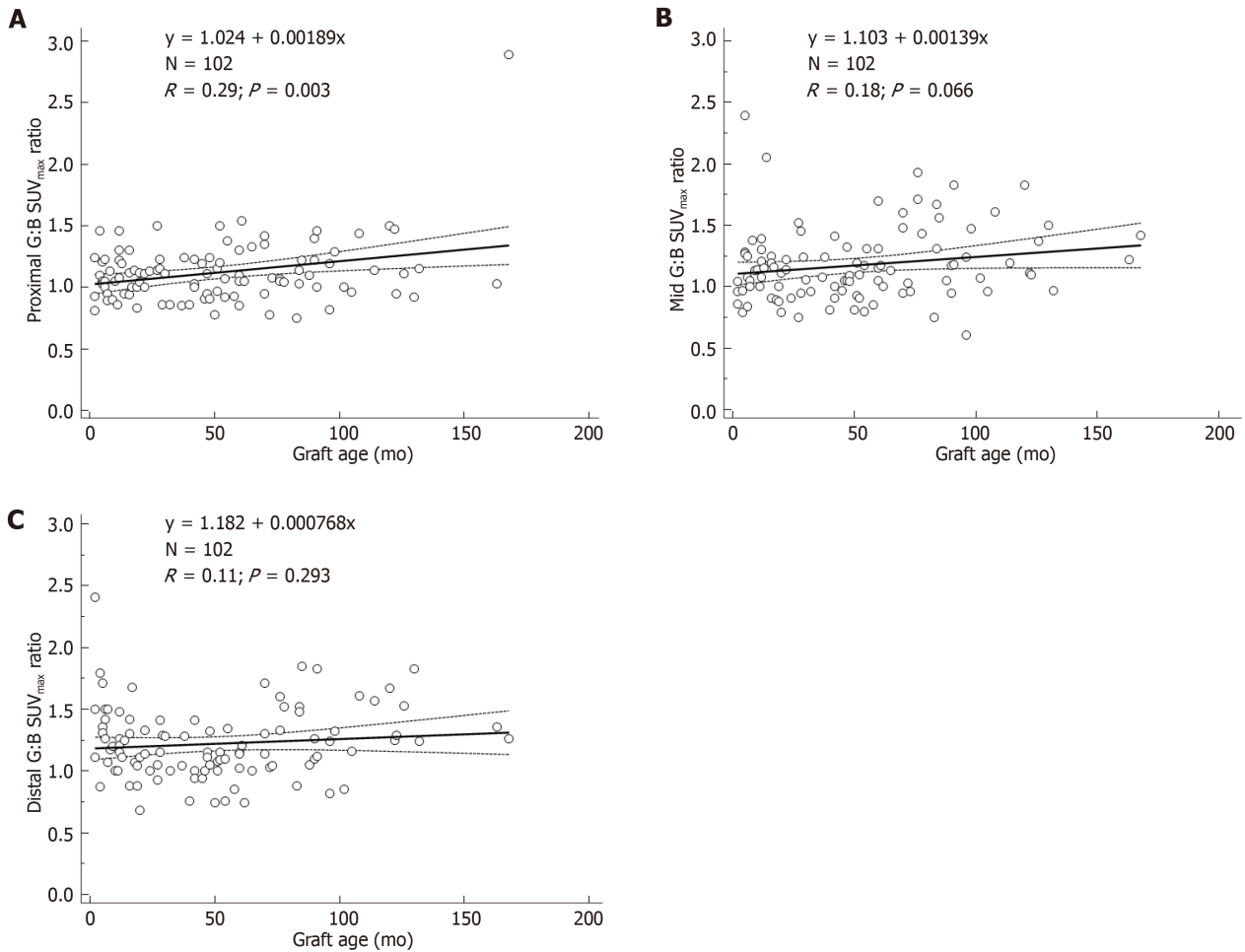
^a*P* < 0.05 versus "Diffuse".

Table 5 Frequency of visual uptake patterns and uptake ratios analyzed by graft type

Visual uptake pattern	PT grafts		PTFE grafts	
	<i>n</i>	Uptake ratio	<i>n</i>	Uptake ratio
Diffuse	85	1.2 ± 0.3	77	1.1 ± 0.2
Focal	2	1.9 ± 0.7 ^a	1	1.5

^a*P* < 0.05 versus "Diffuse".

PT: Polyethylene terephthalate; PTFE: Polytetrafluoroethylene.



DOI: 10.4329/wjr.v15.i8.241 Copyright ©The Author(s) 2023.

Figure 3 Uptake ratios vs graft age in months. A: Proximal regions; B: Mid regions; C: Distal regions of abdominal aortic grafts.

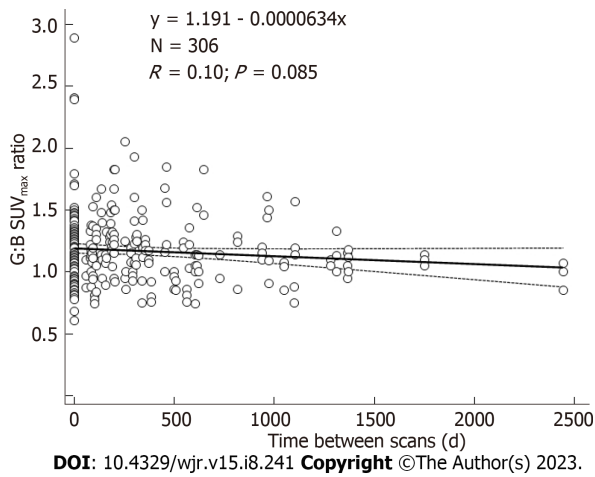


Figure 4 Uptake ratios of abdominal aortic grafts for all patients at all scan times. SUV_{max}: Maximum standardized uptake value.

ARTICLE HIGHLIGHTS

Research background

On [(18)F]fluorodeoxyglucose positron emission tomography/computed tomography (18F-FDG PET/CT), the inflammatory response caused by endoprosthetic stent grafts after endovascular aneurysm repair (EVAR) can show increased 18F-FDG uptake. However, the visual, semiquantitative, and temporal characteristics of uninfected, or aseptic, endovascular aneurysm grafts has not been fully elucidated.

Research motivation

Characterization of aseptic vascular stent grafts on 18F-FDG PET/CT is important to distinguish the normal inflammatory response to graft material *vs* vascular graft infection.

Research objectives

The purpose of this study was to characterize aseptic vascular stent grafts over time.

Research methods

In this observational retrospective cohort study, patients with EVAR who underwent 18F-FDG PET/CT for routine oncologic indications were included. Any patients with suspected or confirmed vascular stent graft infection were excluded. Visual and semiquantitative region of interest (ROI) analysis with maximum standardized uptake value (SUV_{max}) and graft-to-background ascending aorta uptake ratios (URs) of the grafts were obtained. We compared visual analysis and semiquantitative values, grouped by age of grafts, ROI locations, and graft materials.

Research results

Characteristics of an aseptic vascular stent graft on 18F-FDG PET/CT include graft SUV_{max} values within 10%-20% of the ascending aorta background SUV_{max}. The SUV_{max} of older aseptic grafts can be as much as 30% above background. The visual uptake pattern of diffuse, homogeneous uptake less than liver was seen in 98% of aseptic vascular stent grafts.

Research conclusions

Aseptic vascular stent grafts post endovascular repair show mildly increased 18F-FDG uptake, with mean graft-to-background URs of 1.1-1.2. Diffuse homogeneous 18F-FDG uptake less than liver in vascular stent grafts is particularly reassuring as a sign of an uninfected graft.

Research perspectives

This study reinforces prior research in characterizing aseptic vascular grafts on 18F-FDG PET/CT.

FOOTNOTES

Author contributions: Bennett P and Nichols KJ wrote the manuscript; Palestro C, Nichols KJ, and Tomas MB designed the research study; Tomas MB performed image analysis and chart review; Koch CF performed chart review; Nichols KJ, Tomas MB and Palestro C analyzed the data; and all authors have read and approved the final manuscript.

Institutional review board statement: Our Institutional Review Board approved this retrospective study. All data were handled in compliance with the Health Insurance Portability and Accountability Act of 1996.

Informed consent statement: The requirement to obtain informed consent was waived.

Conflict-of-interest statement: All the authors report no relevant conflicts of interest for this article.

Data sharing statement: The original anonymous dataset is available upon reasonable request from the corresponding author at pbennett1@northwell.edu.

Open-Access: This article is an open-access article that was selected by an in-house editor and fully peer-reviewed by external reviewers. It is distributed in accordance with the Creative Commons Attribution NonCommercial (CC BY-NC 4.0) license, which permits others to distribute, remix, adapt, build upon this work non-commercially, and license their derivative works on different terms, provided the original work is properly cited and the use is non-commercial. See: <https://creativecommons.org/licenses/by-nc/4.0/>

Country/Territory of origin: United States

ORCID number: Paige Bennett 0009-0002-4639-0481; Maria Bernadette Tomas 0000-0002-3858-2347; Christopher F Koch 0000-0002-8339-8362; Kenneth J Nichols 0000-0003-2010-7078; Christopher J Palestro 0000-0002-5998-832X.

S-Editor: Wang JJ

L-Editor: A

P-Editor: Wang JJ

REFERENCES

- Casali M, Lauri C, Altini C, Bertagna F, Cassarino G, Cistaro A, Erba AP, Ferrari C, Mainolfi CG, Palucci A, Prandini N, Baldari S, Bartoli F, Bartolomei M, D'Antonio A, Dondi F, Gandolfo P, Giordano A, Laudicella R, Massollo M, Nieri A, Piccardo A, Vendramin L, Muratore F, Lavelli V, Albano D, Burrioni L, Cuocolo A, Evangelista L, Lazzeri E, Quartuccio N, Rossi B, Rubini G, Sollini M, Versari A, Signore A. State of the art of (18)F-FDG PET/CT application in inflammation and infection: a guide for image acquisition and interpretation. *Clin Transl Imaging* 2021; **9**: 299-339 [PMID: 34277510 DOI: 10.1007/s40336-021-00445-w]
- Arnon-Sheleg E, Keidar Z. Vascular Graft Infection Imaging. *Semin Nucl Med* 2023; **53**: 70-77 [PMID: 36104271 DOI: 10.1053/j.semnuclmed.2022.08.006]
- Bowles H, Ambrosioni J, Mestres G, Hernández-Meneses M, Sánchez N, Llopis J, Yugueros X, Almela M, Moreno A, Rimbau V, Fuster D, Miró JM; Hospital Clinic Endocarditis Study Group. Diagnostic yield of (18)F-FDG PET/CT in suspected diagnosis of vascular graft infection: A prospective cohort study. *J Nucl Cardiol* 2020; **27**: 294-302 [PMID: 29907934 DOI: 10.1007/s12350-018-1337-1]
- Chrapko BE, Chrapko M, Nocuń A, Zubilewicz T, Stefaniak B, Mitura J, Wolski A, Terelecki P. Patterns of vascular graft infection in 18F-FDG PET/CT. *Nucl Med Rev Cent East Eur* 2020; **23**: 63-70 [PMID: 33007092 DOI: 10.5603/NMR.a2020.0015]
- Schaeffers JF, Donas KP, Panuccio G, Kasprzak B, Heine B, Torsello GB, Osada N, Usai MV. Outcomes of Surgical Explantation of Infected Aortic Grafts After Endovascular and Open Abdominal Aneurysm Repair. *Eur J Vasc Endovasc Surg* 2019; **57**: 130-136 [PMID: 30146325 DOI: 10.1016/j.ejvs.2018.07.021]
- Sarrazin JF, Trottier M, Tessier M. How useful is 18F-FDG PET/CT in patients with suspected vascular graft infection? *J Nucl Cardiol* 2020; **27**: 303-304 [PMID: 30046981 DOI: 10.1007/s12350-018-1377-6]
- Jamar F, Buscombe J, Chiti A, Christian PE, Delbeke D, Donohoe KJ, Israel O, Martin-Comin J, Signore A. EANM/SNMMI guideline for 18F-FDG use in inflammation and infection. *J Nucl Med* 2013; **54**: 647-658 [PMID: 23359660 DOI: 10.2967/jnumed.112.112524]
- Reinders Folmer EI, Von Meijenfildt GCI, Van der Laan MJ, Glaudemans AWJM, Slart RHJA, Saleem BR, Zeebregts CJ. Diagnostic Imaging in Vascular Graft Infection: A Systematic Review and Meta-Analysis. *Eur J Vasc Endovasc Surg* 2018; **56**: 719-729 [PMID: 30122333 DOI: 10.1016/j.ejvs.2018.07.010]
- Mahmoodi Z, Salarzaei M, Sheikh M. Prosthetic vascular graft infection: A systematic review and meta-analysis on diagnostic accuracy of 18FDG PET/CT. *Gen Thorac Cardiovasc Surg* 2022; **70**: 219-229 [PMID: 34309812 DOI: 10.1007/s11748-021-01682-6]
- Rojas D, Kontopodis N, Antoniou SA, Ioannou CV, Antoniou GA. 18F-FDG PET in the Diagnosis of Vascular Prosthetic Graft Infection: A Diagnostic Test Accuracy Meta-Analysis. *Eur J Vasc Endovasc Surg* 2019; **57**: 292-301 [PMID: 30241981 DOI: 10.1016/j.ejvs.2018.08.040]
- Keidar Z, Pirmisashvili N, Leiderman M, Nitecki S, Israel O. 18F-FDG uptake in noninfected prosthetic vascular grafts: incidence, patterns, and changes over time. *J Nucl Med* 2014; **55**: 392-395 [PMID: 24516259 DOI: 10.2967/jnumed.113.128173]
- Liddy S, Mallia A, Collins CD, Killeen RP, Skehan S, Dodd JD, Subesinghe M, Murphy DJ. Vascular findings on FDG PET/CT. *Br J Radiol* 2020; **93**: 20200103 [PMID: 32356457 DOI: 10.1259/bjr.20200103]
- Tsuda K, Washiyama N, Takahashi D, Natsume K, Ohashi Y, Hirano M, Takeuchi Y, Shiiya N. 18-Fluorodeoxyglucose positron emission tomography in the diagnosis of prosthetic aortic graft infection: the difference between open and endovascular repair. *Eur J Cardiothorac Surg* 2022; **63** [PMID: 36394268 DOI: 10.1093/ejcts/ezac542]
- Kim A, Koshevarova V, Shure A, Joseph S, Villanueva-Meyer J, Bhargava P. FDG PET/CT in abdominal aortic graft infection: A case report and literature review. *Radiol Case Rep* 2023; **18**: 27-30 [PMID: 36324849 DOI: 10.1016/j.radcr.2022.09.106]
- Rahimi M, Adlouni M, Ahmed AI, Alnabelsi T, Chinnadurai P, Al-Mallah MH. Diagnostic Accuracy of FDG PET for the Identification of Vascular Graft Infection. *Ann Vasc Surg* 2022; **87**: 422-429 [PMID: 35760267 DOI: 10.1016/j.avsg.2022.05.029]

Rare portal hypertension caused by Abernethy malformation (Type IIC): A case report

Xin Yao, Yang Liu, Li-Dan Yu, Jian-Ping Qin

Specialty type: Gastroenterology and hepatology

Provenance and peer review: Unsolicited article; Externally peer reviewed.

Peer-review model: Single blind

Peer-review report's scientific quality classification

Grade A (Excellent): 0
Grade B (Very good): 0
Grade C (Good): C
Grade D (Fair): D
Grade E (Poor): 0

P-Reviewer: Ghazanfar A, United Kingdom; Pizanias M, United Kingdom

Received: June 16, 2023

Peer-review started: June 16, 2023

First decision: July 19, 2023

Revised: July 23, 2023

Accepted: July 31, 2023

Article in press: July 31, 2023

Published online: August 28, 2023



Xin Yao, Yang Liu, Li-Dan Yu, Jian-Ping Qin, Department of Gastroenterology, General Hospital of Western Theater Command, Chengdu 610083, Sichuan Province, China

Corresponding author: Jian-Ping Qin, MD, Chief Physician, Department of Gastroenterology, General Hospital of Western Theater Command, No. 270 Rongdu Road, Chengdu 610083, Sichuan Province, China. jpqqing@163.com

Abstract

BACKGROUND

Abernethy malformation is a rare congenital vascular malformation with a portosystemic shunt that may clinically manifest as cholestasis, dyspnea, or hepatic encephalopathy, among other conditions. Early diagnosis and classification are very important to further guide treatment. Typically, patients with congenital portosystemic shunts have no characteristics of portal hypertension. Herein, we report an 18-year-old female with prominent portal hypertension that manifested mainly as rupture and bleeding of esophageal varices. Imaging showed a thin main portal vein, no portal vein branches in the liver, and bleeding of the esophageal and gastric varices caused by the collateral circulation upwards from the proximal main portal vein. Patients with Abernethy malformation type I are usually treated with liver transplantation, and patients with type II are treated with shunt occlusion, surgery, or transcatheter coiling. Our patient was treated with endoscopic surgery combined with drug therapy and had no portal hypertension and good hepatic function for 24 mo of follow-up.

CASE SUMMARY

This case report describes our experience in the diagnosis and treatment of an 18-year-old female with Abernethy malformation type IIC and portal hypertension. This condition was initially diagnosed as cirrhosis combined with portal hypertension. The patient was ultimately diagnosed using liver histology and subsequent imaging, and the treatment was highly effective. To publish this case report, written informed consent was obtained from the patient, including the attached imaging data.

CONCLUSION

Abernethy malformation type IIC may develop portal hypertension, and traditional nonselective beta-blockers combined with endoscopic treatment can achieve high efficacy.

Key Words: Abernethy malformation; congenital absence of portal vein; portal hypertension

©The Author(s) 2023. Published by Baishideng Publishing Group Inc. All rights reserved.

Core Tip: Abernethy malformation is a rare congenital vascular malformation with portosystemic shunts that may clinically manifest as cholestasis, dyspnea, or hepatic encephalopathy, among other conditions. Typically, patients with congenital portosystemic shunts have no characteristics of portal hypertension. We reported an 18-year-old woman with Abernethy malformation type II and portal hypertension. This condition was initially diagnosed as cirrhosis combined with portal hypertension. The patient was ultimately diagnosed by liver puncture and biopsy with subsequent imaging.

Citation: Yao X, Liu Y, Yu LD, Qin JP. Rare portal hypertension caused by Abernethy malformation (Type IIC): A case report. *World J Radiol* 2023; 15(8): 250-255

URL: <https://www.wjgnet.com/1949-8470/full/v15/i8/250.htm>

DOI: <https://dx.doi.org/10.4329/wjr.v15.i8.250>

INTRODUCTION

Among patients accompanied by portal hypertension, Esophageal variceal bleeding is a frequent complication. However, although the prevalence of Abernethy malformation is approximately 1 in 30000–50000 people[1], and it typically presents no characteristics of portal hypertension, this congenital occult disease should not be ignored in clinical practice. As imaging studies have progressed, the diagnosis of Abernethy malformation has increased. The shunts of Abernethy malformation type II most often occur in the main portal vein (MPV) and in the mesenteric, gastric, and splenic veins[2]. To date, no reports have described the shunt entering the splenic hilum through the splenic vein and establishing collateral circulation, which then enters the inferior vena cava (IVC) through the splenorenal shunt. In addition, this patient developed portal hypertension, which was treated effectively.

CASE PRESENTATION

Chief complaints

An 18-year-old woman was admitted to our hospital with a 10-d history of left upper abdominal distension, pain, and discomfort, accompanied by hematemesis.

History of present illness

The patient had no history of present illness.

History of past illness

The patient had no history of past illness.

Personal and family history

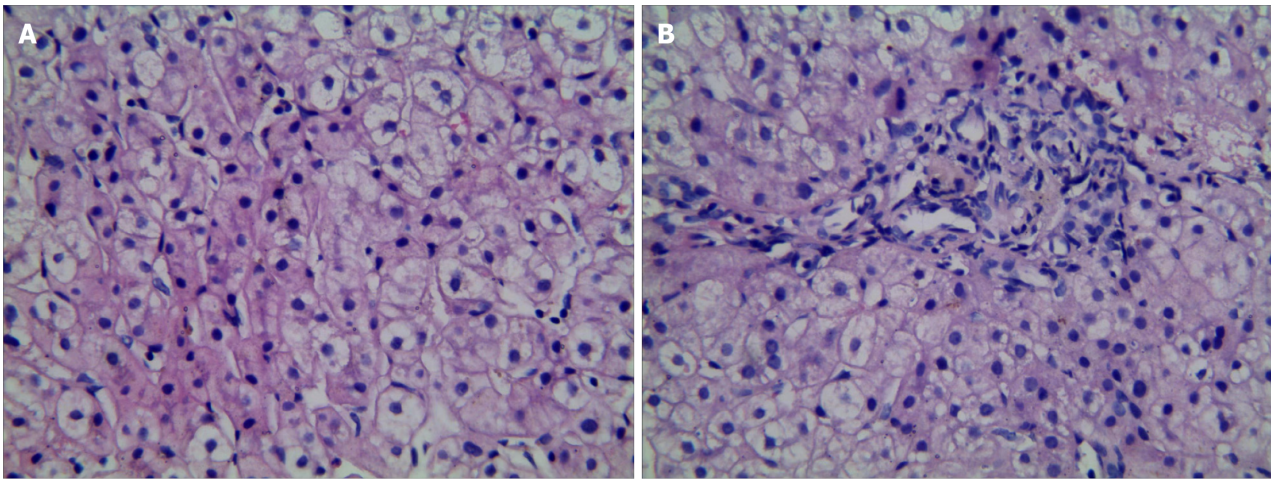
The patient had no special personal history or family history.

Physical examination

Physical examination showed no abnormalities, except for the spleen palpable 2 cm below the left costal margin.

Laboratory examinations

On routine blood tests, the hematocrit was 25.6%, the hemoglobin concentration was 73 g/L, the red blood cell count was $3.71 \times 10^{12}/L$, the platelet count was $152 \times 10^9/L$, and the white blood cell count was $1.31 \times 10^9/L$. The results of laboratory examinations were Child–Pugh grade A liver function. Test results for hepatitis and autoimmune antibodies were negative. Ceruloplasmin was normal. Bone marrow (BM) smear displayed active proliferation of karyocytes, with 59% granulocytes and 22% erythroid cells (granulocytes/erythroid cell ratio of 2.68); most of the mature red blood cells were expanded in the central light-stained area. Active proliferation of BM tissue was shown on BM puncture and biopsy without other special changes. Punctured hepatic tissue. The structure of hepatic lobules was normal, the hepatic sinusoids were not dilated, the diameter of the central vein was generally normal, and the hepatic parenchyma had no obvious inflammatory changes. No portal vein branch entering the hepatic lobule was detected. The number and shape of small bile ducts in the portal area were normal, and the stroma was infiltrated by a small number of chronic inflammatory cells (Figure 1).



DOI: 10.4329/wjr.v15.i8.250 Copyright ©The Author(s) 2023.

Figure 1 The number and shape of small bile ducts in the portal area were normal, and the stroma was infiltrated by a small number of chronic inflammatory cells. A and B: Punctured hepatic tissue with hematoxylin and eosin staining ($\times 400$).

Imaging examinations

Colonoscopy suggested no abnormalities. Gastroscopy revealed severe esophageal varices (type G1OV1). Further imaging with 320-detector row computed tomography (CT) angiography and three-dimensional (3D) reconstruction of the portal vein showed a thin MPV, no portal vein branch in the liver, disordered vessels at the proximal MPV, and esophageal varices caused by collateral circulation upwards at the origin of the portal vein. The superior mesenteric vein and the splenic vein formed a common trunk. After entering the splenic hilum, the splenic vein formed collateral circulation along the lower left side of the vertebral body, resulting in a venous tumor thrombus, and then flowed into the renal vein and returned to the IVC (Figure 2). Ultrasound of the portal vein showed no portal vein branch in the liver, a thin MPV with blood flow, no thrombosis or cavernous transformation, reversed blood flow in the splenic vein, and thickened hepatic arteries suspected to be compensation. Cardiac ultrasound showed no abnormalities.

FINAL DIAGNOSIS

Abernethy malformation type IIC: Portal hypertension.

TREATMENT

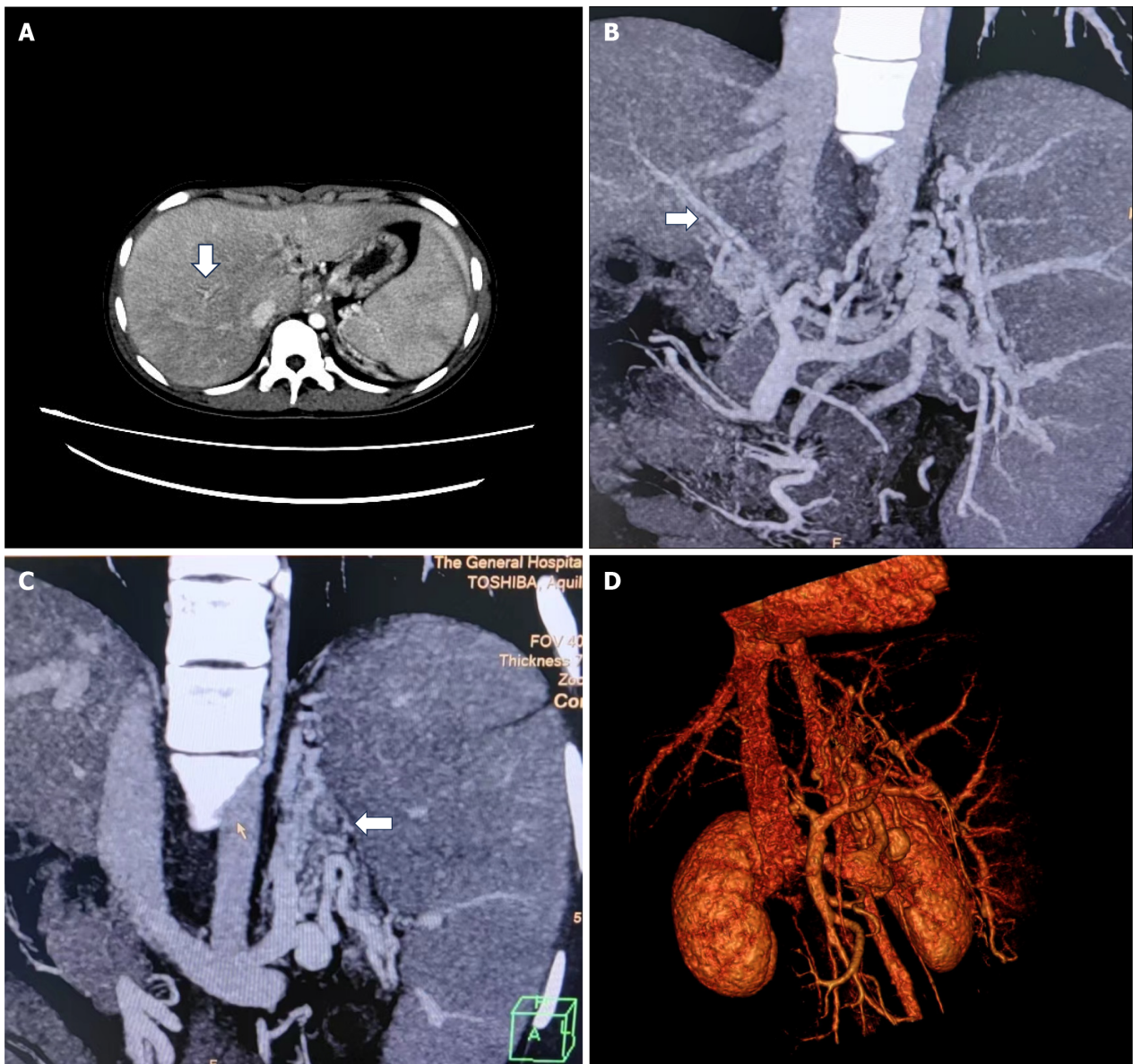
Patients with Abernethy malformation type II can be treated with shunt occlusion and liver transplantation, and the patient selected conservative treatment. After the first endoscopic ligation of esophageal varices, endoscopic treatment was carried out 3 consecutive times at an interval of 1 mo. Simultaneously, 10 mg of oral propranolol hydrochloride was given 3 times/d. The heart rate was controlled at approximately 55 times/min.

OUTCOME AND FOLLOW-UP

Three months later, gastroscopy indicated esophageal varices (mild, RC-) and a local scar after ligation. Thus, 2.5 mg of warfarin per day was administered. The patient was followed up for 24 consecutive months and showed no portal hypertension and Child-Pugh grade A.

DISCUSSION

John Abernethy first reported Abernethy malformation, also known as a congenital extrahepatic portosystemic shunt, in 1793. Abernethy malformation is a rare clinical disease with a prevalence of one case out of 30000–50000[1]. It is characterized by the absence or dysplasia of the portal vein caused by abnormal development of fetal umbilical veins and vitelline veins, with abnormal shunts between the portal vein system and the vena cava system[3]. In 1994, Morgan *et al* [2] defined Abernethy malformation type I as the absence of portal vein flow in the liver caused by the congenital absence of the portal vein. Abernethy malformation type II was defined as a significant reduction in intrahepatic blood flow



DOI: 10.4329/wjr.v15.i8.250 Copyright ©The Author(s) 2023.

Figure 2 After entering the splenic hilum, the splenic vein formed collateral circulation along the lower left side of the vertebral body, resulting in a venous tumor thrombus, and then flowed into the renal vein and returned to the inferior vena cava. A: The main portal vein was thin, and no portal vein branch was found in the liver (arrow); B: The vessels were disordered at the proximal main portal vein, and esophageal varices were caused by collateral circulation upward at the portal vein origin. The superior mesenteric vein and the splenic vein formed a common trunk (arrow); C and D: After entering the splenic hilum, the splenic vein established collateral circulation (forming a venous tumour), flowed into the renal vein and returned to the inferior vena cava (arrow).

caused by a thin MPV. In type I Abernethy malformation patients, the superior mesenteric vein does not merge with the splenic vein, and merging of the superior mesenteric vein with the splenic vein is classified as type Ib. In 2011, Lautz *et al* [4] classified patients with congenital portal vein dysplasia into type IIa (shunt occurring in the left or right portal vein of the liver, including patent ductus venosus), type IIb (shunt occurring in the MPV), and type IIc (shunt occurring in the mesenteric veins, gastric veins, or splenic veins) based on the different anatomical positions of the portosystemic shunts. However, this classification method includes patients with congenital intrahepatic portosystemic shunts and is not widely used.

The clinical manifestations of Abernethy malformation vary greatly, from incidental detection to hepatocerebralopathy and hepatic failure, and depend on the type of abnormality. Patients may be asymptomatic or present with nonspecific symptoms, such as hypergalactosemia, hyperbilirubinemia, and hyperammonemia, due to delayed metabolism of these metabolites in the liver or their metabolism outside of the liver [5,6]. Abernethy malformation may also cause pulmonary venous congestion, leading to hepatopulmonary syndrome, which manifests as dyspnea caused by pulmonary hypertension and even syncope [7]. In addition, Abernethy malformation can be complicated by multiple malformations [2], such as congenital heart disease, skeletal muscle system malformations, and polysplenia. When patients visit with symptoms, including dyspnea and varicose veins of the lower limbs [8], misdiagnosis or missed diagnosis is likely. This patient was admitted due to rupture and bleeding of esophageal varices, which is easily misdia-

gnosed as cirrhotic portal hypertension accompanied by cavernous transformation of the portal vein. Hepatobiliary abnormalities, such as cirrhosis, veno-occlusive disease, noncirrhotic portal fibrosis, and biliary atresia, were excluded based on the percutaneous liver biopsy. A BM smear and biopsy excluded hematological system-related diseases. The thin portal vein and no portal vein branches in the liver indicated Abernethy malformation. However, CT showed a similar cavernous transformation at the proximal portal vein, so Abernethy malformation needed to be differentiated from extrahepatic portal vein obstruction-related diseases.

Imaging is the preferred diagnostic method for Abernethy malformations. Abdominal ultrasound can be used as a preliminary screening tool. Portal vein CT angiography and 3D reconstruction can help identify abnormal development of the portal vein and the anatomy of extrahepatic shunts in Abernethy malformations. Webb *et al*[9] described the ultrasound display of the portal vein in Abernethy malformations as an intact empty hepatic hilum with portal vein block appearing as a wide, rhombic high-level echo band. Patients with congenital portosystemic shunts do not have characteristics of portal hypertension, such as splenomegaly, varicosity, and collateral branches[10]. A recent study[11] suggested that acquired extrahepatic portosystemic shunts are usually detected in patients with cirrhosis. In addition, noncirrhotic portal vein thrombosis may also present manifestations similar to Abernethy malformation. In this patient, an ultrasound of the portal vein showed no portal vein branches in the liver, thrombosis, or cavernous transformation but showed thin MPV with visible blood flow signals and reversed blood flow in the splenic vein. Although the CT of this patient showed a similar cavernous transformation in the MPV, the author's team believes that extrahepatic portal vein obstruction caused by chronic thrombosis and cavernous transformation of the portal vein was excluded by ultrasound. No shunt between the portal vein and the splenic vein was detected, but after entering the splenic hilum, the blood flowed back to the IVC in the form of a thick "spleen kidney" shunt through the collateral circulation, which is different from the usual form of Abernethy syndrome and may be another manifestation of Abernethy malformation type IIC. Several studies[12, 13] showed that various congenital malformations are related to Abernethy malformation, and cardiac abnormalities are the most common. This patient presented with no abnormalities on cardiac ultrasound, so cardiac malformations could be excluded. We speculate that this patient may have a congenital hypoplastic portal vein system. Because of the thin MPV and no portal vein branch, the "splenorenal communicating branch" that should degenerate during development continued to exist chronically. The blood flow returning to the liver was blocked at the portal vein origin, forming regional portal hypertension (consistent with the appearance of abundant capillary collateral circulation around the MPV origin on CT, which is similar to cavernous transformation). In addition, the blood flow of the splenic vein was reversed, causing splenic congestion and swelling, and then returned to the IVC through the splenic-renal communicating branch.

Hepatic damage in patients with Abernethy malformations is milder than the damage in patients with cirrhosis, and the increases in bilirubin and aminophenase are often not obvious[14]. This patient's hepatic function was normal, with no hepatic encephalopathy, which is in line with previous research results[5,15]. Most patients with Abernethy malformations have elevated blood ammonia, but fewer patients present with hepatic encephalopathy. Although the thin portal vein may lead to insufficient blood flow to the liver, the hepatic artery may play a compensatory role in the long-term course of the disease, which is consistent with hepatic artery thickening on portal ultrasound and compensatory performance.

Liver transplantation is the main treatment method for Abernethy malformation type I. Patients with Abernethy malformation type II are treated with shunt occlusion and liver transplantation[6,16]. The choice of an interventional or surgical method is based on the degree of extrahepatic portosystemic shunts, the anatomical position of shunts, and the diameter of the shunts. The liver tumors, hepatopulmonary syndrome, and hyperammonemia disappear after the occlusion of the abnormal shunts[4,15]. Portal hypertension caused by Abernethy malformation has not been reported; thus, we first recommended liver transplantation for this patient, and the patient finally chose conservative treatment. Endoscopic ligation may aggravate portal hypertension, slow portal vein blood flow, and form thrombi[17]. Therefore, nonselective beta-blockers and anticoagulant drugs were added. After 24 mo of follow-up, the patient presented with no complications of portal hypertension or portal thrombosis and good hepatic function. We will continue to monitor this patient.

CONCLUSION

Abernethy malformation type IIC may cause portal hypertension, and combining traditional nonselective beta-blockers with endoscopic therapy is an effective treatment.

FOOTNOTES

Author contributions: Yao X wrote the paper; Liu Y collected the data; Yu LD collected the data; Qin JP participated in and guided the operation, conceptualized the idea, and finalized the manuscript.

Informed consent statement: Informed written consent was obtained from the patient for publication of this report and any accompanying images.

Conflict-of-interest statement: All the authors declare that they have no conflict of interests to report.

CARE Checklist (2016) statement: The authors have read the CARE Checklist (2016), and the manuscript was prepared and revised

according to the CARE Checklist (2016).

Open-Access: This article is an open-access article that was selected by an in-house editor and fully peer-reviewed by external reviewers. It is distributed in accordance with the Creative Commons Attribution NonCommercial (CC BY-NC 4.0) license, which permits others to distribute, remix, adapt, build upon this work non-commercially, and license their derivative works on different terms, provided the original work is properly cited and the use is non-commercial. See: <https://creativecommons.org/licenses/by-nc/4.0/>

Country/Territory of origin: China

ORCID number: Xin Yao 0000-0002-9977-6153; Yang Liu 0000-0003-1700-3890; Li-Dan Yu 0000-0001-5261-2496; Jian-Ping Qin 0000-0001-7834-8830.

S-Editor: Liu JH

L-Editor: A

P-Editor: Zhao S

REFERENCES

- 1 **Abernethy J.** Account of Two Instances of Uncommon Formation in the Viscera of the Human Body: From the Philosophical Transactions of the Royal Society of London. *Med Facts Obs* 1797; **7**: 100-108 [PMID: 29106224]
- 2 **Morgan G,** Superina R. Congenital absence of the portal vein: two cases and a proposed classification system for portasystemic vascular anomalies. *J Pediatr Surg* 1994; **29**: 1239-1241 [PMID: 7807356 DOI: 10.1016/0022-3468(94)90812-5]
- 3 **Peček J,** Fister P, Homan M. Abernethy syndrome in Slovenian children: Five case reports and review of literature. *World J Gastroenterol* 2020; **26**: 5731-5744 [PMID: 33088165 DOI: 10.3748/wjg.v26.i37.5731]
- 4 **Lautz TB,** Tantemsapya N, Rowell E, Superina RA. Management and classification of type II congenital portosystemic shunts. *J Pediatr Surg* 2011; **46**: 308-314 [PMID: 21292079 DOI: 10.1016/j.jpedsurg.2010.11.009]
- 5 **Ponziani FR,** Faccia M, Zocco MA, Giannelli V, Pellicelli A, Ettorre GM, De Matthaeis N, Pizzolante F, De Gaetano AM, Riccardi L, Pompili M, Rapaccini GL. Congenital extrahepatic portosystemic shunt: description of four cases and review of the literature. *J Ultrasound* 2019; **22**: 349-358 [PMID: 30357760 DOI: 10.1007/s40477-018-0329-y]
- 6 **Uchida H,** Sakamoto S, Kasahara M, Kudo H, Okajima H, Nio M, Umeshita K, Ohdan H, Egawa H, Uemoto S; Japanese Liver Transplantation Society. Longterm Outcome of Liver Transplantation for Congenital Extrahepatic Portosystemic Shunt. *Liver Transpl* 2021; **27**: 236-247 [PMID: 32463947 DOI: 10.1002/lt.25805]
- 7 **Lin XQ,** Rao JY, Xiang YF, Zhang LW, Cai XL, Guo YS, Lin KY. Case Report: A Rare Syncope Case Caused by Abernethy II and a Review of the Literature. *Front Cardiovasc Med* 2021; **8**: 784739 [PMID: 35059447 DOI: 10.3389/fcvm.2021.784739]
- 8 **Wang W,** Li Q, Wen L. An Unusual Cause of Left Lower Extremity Varicose Veins. *Gastroenterology* 2022; **162**: e9-e11 [PMID: 34390728 DOI: 10.1053/j.gastro.2021.08.010]
- 9 **Webb LJ,** Berger LA, Sherlock S. Grey-scale ultrasonography of portal vein. *Lancet* 1977; **2**: 675-677 [PMID: 71493 DOI: 10.1016/s0140-6736(77)90492-5]
- 10 **Ghuman SS,** Gupta S, Buxi TB, Rawat KS, Yadav A, Mehta N, Sud S. The Abernethy malformation-myriad imaging manifestations of a single entity. *Indian J Radiol Imaging* 2016; **26**: 364-372 [PMID: 27857464 DOI: 10.4103/0971-3026.190420]
- 11 **Kumar P,** Bhatia M, Garg A, Jain S, Kumar K. Abernethy malformation: A comprehensive review. *Diagn Interv Radiol* 2022; **28**: 21-28 [PMID: 34914605 DOI: 10.5152/dir.2021.20474]
- 12 **Kim ES,** Lee KW, Choe YH. The Characteristics and Outcomes of Abernethy Syndrome in Korean Children: A Single Center Study. *Pediatr Gastroenterol Hepatol Nutr* 2019; **22**: 80-85 [PMID: 30671377 DOI: 10.5223/pghn.2019.22.1.80]
- 13 **Ponziani FR,** Faccia M, Zocco MA, Giannelli V, Pellicelli A, Ettorre GM, De Matthaeis N, Pizzolante F, De Gaetano AM, Riccardi L, Pompili M, Rapaccini GL. Congenital extrahepatic portosystemic shunt: description of four cases and review of the literature. *J Ultrasound* 2019; **22**: 349-358 [PMID: 30357760 DOI: 10.1007/s40477-018-0329-y]
- 14 **Alonso-Gamarra E,** Parrón M, Pérez A, Prieto C, Hierro L, López-Santamaría M. Clinical and radiologic manifestations of congenital extrahepatic portosystemic shunts: a comprehensive review. *Radiographics* 2011; **31**: 707-722 [PMID: 21571652 DOI: 10.1148/rg.313105070]
- 15 **Zhou M,** Zhang J, Luo L, Wang B, Zheng R, Li L, Jing H, Zhang S. Surgical Ligation for the Treatment of an Unusual Presentation of Type II Abernethy Malformation. *Ann Vasc Surg* 2020; **65**: 285.e1-285.e5 [PMID: 31705994 DOI: 10.1016/j.avsg.2019.10.094]
- 16 **Tanaka H,** Saijo Y, Tomonari T, Tanaka T, Taniguchi T, Yagi S, Okamoto K, Miyamoto H, Sogabe M, Sato Y, Muguruma N, Tsuneyama K, Sata M, Takayama T. An Adult Case of Congenital Extrahepatic Portosystemic Shunt Successfully Treated with Balloon-occluded Retrograde Transvenous Obliteration. *Intern Med* 2021; **60**: 1839-1845 [PMID: 33456037 DOI: 10.2169/internalmedicine.5914-20]
- 17 **Wang L,** Guo X, Shao X, Xu X, Zheng K, Wang R, Chawla S, Basaranoglu M, Qi X. Association of endoscopic variceal treatment with portal venous system thrombosis in liver cirrhosis: a case-control study. *Therap Adv Gastroenterol* 2022; **15**: 17562848221087536 [PMID: 35574427 DOI: 10.1177/17562848221087536]



Published by **Baishideng Publishing Group Inc**
7041 Koll Center Parkway, Suite 160, Pleasanton, CA 94566, USA

Telephone: +1-925-3991568

E-mail: bpgoffice@wjgnet.com

Help Desk: <https://www.f6publishing.com/helpdesk>

<https://www.wjgnet.com>

